

Hindawi Publishing Corporation
Advances in OptoElectronics
Volume 2008, Article ID 373259, 5 pages
doi:10.1155/2008/373259

Research Article

Optical Intensity Modulation in an LiNbO₃ Slab-Coupled Waveguide

Yalin Lu¹ and Kitt Reinhardt²

¹Laser and Optics Research Center (LORC), Department of Physics, United States Air Force Academy, CO 80840, USA

²Air Force Office of Scientific Research (AFOSR)/NE, 875 North Randolph Street, Suite 326, Arlington, VA 22203, USA

Correspondence should be addressed to Yalin Lu, yalin.lu@usafa.edu

Received 29 September 2008; Accepted 3 December 2008

Recommended by Jung Huang

Optical intensity modulation has been demonstrated through switching the optical beam between the main core waveguide and a closely attached leaky slab waveguide by applying a low-voltage electrical field. Theory for simulating such an LiNbO₃ slab-coupled waveguide structure was suggested, and the result indicates the possibility of making the spatial guiding mode large, circular and symmetric, which further allows the potential to significantly reduce the coupling losses with adjacent lasers and optical networks. Optical intensity modulation using electro-optic effect was experimentally demonstrated in a 5 cm long waveguide fabricated by using a procedure of soft proton exchange and then an overgrowth of thin LN film on top of a c-cut LiNbO₃ wafer.

Copyright © 2008 Y. Lu and K. Reinhardt. This is an open access article distributed under the Creative Commons Attribution License, which permits unrestricted use, distribution, and reproduction in any medium, provided the original work is properly cited.

1. Introduction

High-speed optical modulation by microwave and millimeter-wave signals is useful in many optoelectronics and microwave photonics applications, including long-haul optical communication systems, radio frequency-over-fiber (ROF) for transferring mobile RF signals, optical measurement, and high-resolution coherence spectroscopy. A typical optical intensity modulation for such ROF applications is the single-sideband modulation having a basic operation principle through mixing two balanced-phase-modulated light beams driven by a pair of RF signals with a phase shift of $\pi/2$ [1]. These used optical modulators usually have very complicated structures, because of the involvement of at least two fast electro-optic (EO) modulators, a pair of RF modulation sources, and a set of fine tuning electronics. Such subsystems' overall performances are primarily limited by the used fast EO modulators, mainly characterized by their half-wave voltage and insertion loss—a combined term of them is defined as the modulation efficiency.

The majority of fast optical modulators are relying on using EO effect in ferroelectric oxide crystals such as LiNbO₃ (LN), LiTaO₃ (LT), and EO ceramics [2], which are able to render extremely fast response speeds in the range from nano-to-picosecond and an ultrawide wavelength

bandwidth over a few hundred nanometers [3]. EO guided-wave modulators have been becoming very important in integrated optoelectronics, following a tremendous number of studies and publications in about the past four decades. Recently, high-speed and low-voltage LN traveling-wave electrode intensity modulators operated at 40 Gbps with a half-wave voltage of ~ 1 V have been reported [4].

In general, a guided-wave LN EO modulator includes a Mach-Zehnder (MZ) waveguide interferometer composing of two “Y” branches, a section of parallel waveguides connecting the two “Y” branches, and an electrode layout suitable for a specific performance requirement. Waveguides are normally buried supporting a single propagation mode, and were fabricated by either titanium-indiffusion or proton exchanging (PE) methods. Pure ridge-type waveguides are less useful in real cases, because of the high propagation loss associated with the microfabricated ridge's boundaries. Electrode layout can be very versatile too. They can be right on top of the guide, or aside the guide, or using the traveling-wave design, and so forth. No matter what designs discussed above that will be used, the majority of past EO guide modulators are relying on the principle of modulating optical phase, which requires the device to reach the so-called half-wave voltage, $V_\pi = \lambda d / (n^3 \gamma L)$. Here d is the electrode spacing, λ the wavelength, γ the EO coefficient, and L the

interaction length. The full modulation thus corresponds to a 90° rotation of the incident light's polarization plane by the applied electrical field. Apparently, tough challenges will find the way to further reduce the modulation voltage.

High insertion loss is also a "hard-to-avoid" issue, which is almost intrinsic to currently used waveguide designs and those associated fabrications. For example, usually both titanium-indiffusion and proton exchange create a relatively large index difference ($\delta n \sim 0.02$), which will confine the fundamental mode in a small core size of only about a few microns. Because indiffusion/exchanging methods are normally unidirectional (normal to the wafer's surface), it clearly lacks a capability to fabricate a waveguide having circular and symmetric core. Smallness and asymmetry of common waveguide cores have been found to account for a large portion of the measured high insertion losses, when coupling them to the common optical networks or pumping diode lasers.

In this research, a new intensity modulation mechanism, which has the potential to use a very low driving electrical voltage, was investigated. This modulation principle involves leaking the light from the main guiding core to an attached leaky slab waveguide through slightly changing the beam's polarization orientation by the applied electrical field. Realization of this function will rely on designing such a slab-coupled waveguide (SCW) structure. Additionally, this SCW structure has the potential to offer a large, circular, and symmetric beam profile for propagating the single-spatial-mode, which therefore further provides the possibility to significantly reduce the coupling losses. In the following sections of this paper, preliminary SCW design/simulation, initial fabrication of such SCW on LiNbO_3 crystals, and experimental demonstration of the optical intensity modulation will be introduced.

2. The SCW Design Using LN Crystal

In recent years, a new kind of diode lasers, referred to as slab-coupled optical waveguide lasers, has been demonstrated mainly for outputting near infrared wavelengths [5]. Characteristics of such diode lasers are their large and symmetric single-spatial-mode outputs that can reach a few *Watts*. The slab-coupled waveguide (SCW) concept is actually derived from Marcattili's coupled-mode analysis, which shows that a large passive multimode guide could be designed to operate in a single-spatial-mode by coupling all the higher-order modes to an adjacent slab [6]. In this research, this new SCW concept will be attempted to be used in the LiNbO_3 crystal, in order to expand the crystal's potential for more efficient EO applications.

Figure 1 shows a schematic of a possible SCW design using a z-cut LN followed by two epilayers. Inside the SCW, the main channel waveguide will be buried by a slab waveguide, and the slab is then laterally confined by two etched drains deep into the second epilayer. Vertically, this SCW has a uniform LiNbO_3 substrate layer with an index of n_3 , a uniform core epilayer with an index of n_1 and a layer thickness of h , and a uniform slab epilayer with an index of n_2 and a thickness of l . The difference among the

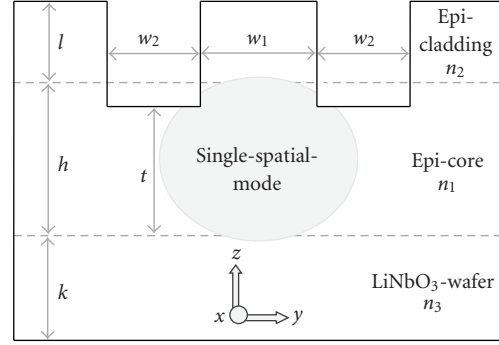


FIGURE 1: Schematic of the LN SCW design.

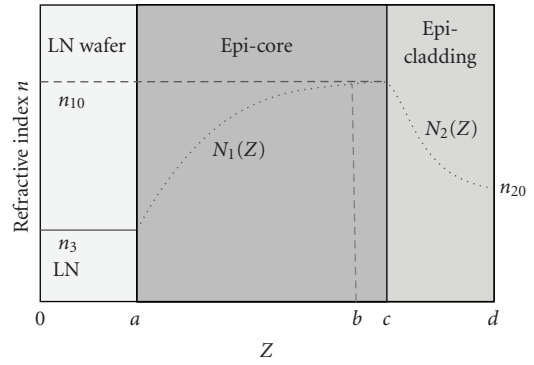


FIGURE 2: Index profile along the c -axis of the LN SCW structure.

three refractive indices should be small and should satisfy $n_3 < n_2 < n_1$. Figure 2 shows an anticipated index profile for such SCW, in which each individual profile of n_3 , n_1 , and n_2 is assumed to be varying (simulating the real PE fabrication conditions). The refractive index profile of the structure can then be written as

$$n^2(z) = \begin{cases} n_3^2, & 0 \leq z \leq a, \\ n_1^2(z) = (n_{10} - n_3) \exp[-\{(b-a-z)/(b-a)\}^r], & a \leq z \leq b, \\ n_{10}^2, & b \leq z \leq c, \\ n_{20}^2 - (n_{20}^2 - n_{10}^2) \left[\frac{d/c - z/c}{d/c - 1} \right]^q, & c \leq z \leq d, \\ 1, & d \leq z, \end{cases} \quad (1)$$

where r and q are profile parameters used to adjust the similarity of the theoretical profiles and actual index profiles inside each epilayer.

By carefully selecting both vertical and lateral confinement conditions, the waveguide can be designed leaky to all high-order modes (complex propagation constants), and guiding only to the fundamental spatial mode. Depending on the cladding index profile, the fundamental spatial mode can be either slightly leaky (its loss is much smaller than that of high-order modes. Therefore, it is loosely guided but has a complex propagation constant too) or fully guided (a real propagation constant). Such propagation constants can

be calculated with the transfer-matrix method (TMM) [7], where the graded-index profile in (1) is approximated by a stair-case profile.

To implement the TMM, the refractive index profile of the structure is divided into a large number of homogeneous layers. The electric field in the i th layer with a refractive index n_i and width d_i can be written as

$$E_i = \begin{cases} C_i \cos [k_i(z - d_{i+1})] + D_i \sin [k_i(z - d_{i+1})], & k_i^2 > 0, \\ C_i \cosh [k_i(z - d_{i+1})] + D_i \sinh [k_i(z - d_{i+1})], & k_i^2 < 0, \end{cases} \quad (2)$$

where $k_i = |k_i|$, $k_i^2 = k_0^2(n_i^2 - n_{\text{eff}}^2)$, $k_0 = 2\pi/\lambda$ is the free-space wave number, and $n_{\text{eff}} = \beta/k_0$ is the effective index of the mode with β being the propagation constant. By applying suitable boundary conditions at the interface between the i th and $(i + 1)$ th layers, the field coefficients, C_i , D_i , C_{i+1} , and D_{i+1} , are related by a 2×2 matrix

$$\begin{pmatrix} C_{i+1} \\ D_{i+1} \end{pmatrix} = S_i \begin{pmatrix} C_i \\ D_i \end{pmatrix}, \quad (3)$$

where S_i is known as the transfer matrix of the i th layer, and for TM and TE modes, it is given differently. For the TE mode, for example, S_i is given by

$$s_i = \begin{cases} \begin{pmatrix} \cos \Delta_{i+1} & -\left(\frac{k_i}{k_{i+1}}\right) \sin \Delta_{i+1} \\ \sin \Delta_{i+1} & \left(\frac{k_i}{k_{i+1}}\right) \cos \Delta_{i+1} \end{pmatrix}, & k_i^2 > 0, \\ \begin{pmatrix} \cosh \Delta_{i+1} & \left(\frac{k_i}{k_{i+1}}\right) \sinh \Delta_{i+1} \\ \sinh \Delta_{i+1} & \left(\frac{k_i}{k_{i+1}}\right) \cosh \Delta_{i+1} \end{pmatrix}, & k_i^2 < 0, \end{cases} \quad (4)$$

where $\Delta_i = k_i(d_i - d_{i+1})$. The field coefficients of the last layer can be related to those of the first layer by simply multiplying the transfer matrices of all layers. Following those standard procedures, we can obtain an eigenvalue equation for the propagation constant β , that is, $F(\beta) = 0$. In general, the propagation constant can be expressed as $\beta = \beta_r + \beta_i$ with β_r being the real part and β_i the imaginary part. A plot of $1/|F|^2$ with β shows a number of resonance peaks, each of which corresponds to a mode. These peaks are Lorentzian in shape. The value of β corresponding to the resonance peak gives the real part of the propagation constant and the FWHM of the Lorentzian gives the imaginary part. In this way, both real and imaginary parts of β can be calculated. The device designing effort should focus on finding both material and structural parameters for best understanding dispersion, phase and attenuation constant of the wave supported in both main and leaky waveguides. However, the optimization procedure is laborious in simulation, and the results are anticipated to be published separately.

For simplicity and by a few times of fitting with LiNbO₃'s refractive indices and the SCW's structural parameters, in Figure 3 we show a preliminary single-spatial-mode simulated at the telecommunication wavelength of 1.55 μm in the

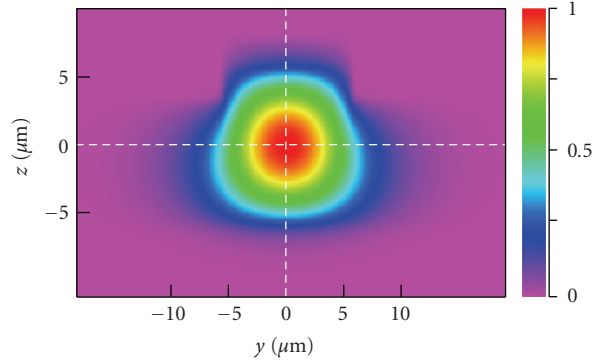


FIGURE 3: A simulated single-spatial-mode guided in a LN SCW having parameters of $h = 9 \mu\text{m}$, $t = 8.4 \mu\text{m}$, $l = 1.0 \mu\text{m}$, $w = 10.0 \mu\text{m}$, $n_2 = 2.13$ and $n_1 = 2.15$.

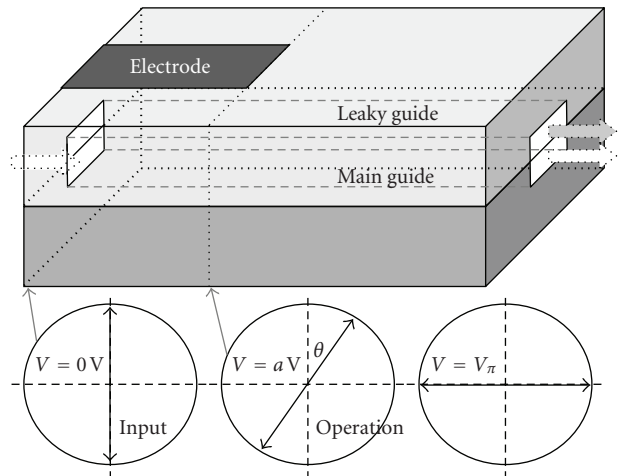


FIGURE 4: New modulation mechanism using the main and the leaky waveguides (top); when applying an electrical field, the polarization rotates along the propagation. The propagation in the main guide therefore leaks to the leaky guide; and the voltage requirement for such a leakage is low, and can be much lower than the common V_π in all phase modulated schemes (bottom).

LN SCW, when we select parameters of $h = 9 \mu\text{m}$, $t = 8.4 \mu\text{m}$, $l = 1.0 \mu\text{m}$, $w = 10.0 \mu\text{m}$, $n_2 = 2.13$, and $n_1 = 2.15$. This mode shows a reasonably symmetric and a large profile of $\sim 15 \times 13 \mu\text{m}^2$, which is actually much larger than that from a common single mode LN waveguide.

3. Intensity Modulation Using the Leaky Mode

Figure 4 shows a schematic of the new intensity modulation principle, in which at the entrance the single-spatial-mode polarization is aligned vertically (as in Figure 1) is fully supported by the main guide (guiding). When rotating the polarization in the incident plane via an applied electrical field, the mode becomes leaky and flows to the leaky slab guide, due to the weakening optical confinement after rotating the incident polarization. When measuring the output from the main guide, an efficient intensity modulation is

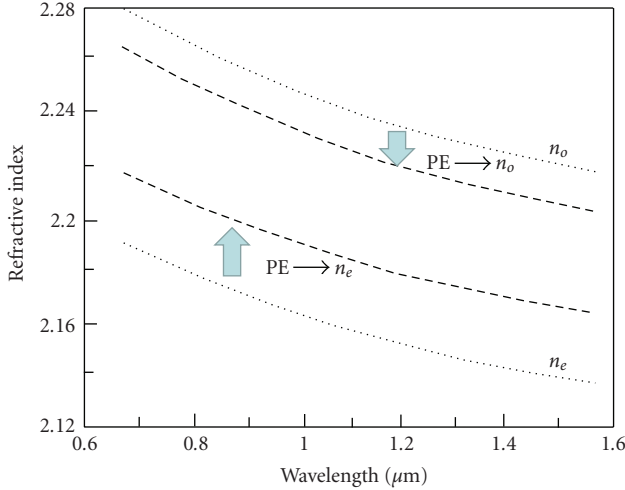


FIGURE 5: Refractive index variations before and after the proton exchanging in LN crystal.

therefore achieved. In this case, only a few degrees of the incident polarization rotation would be needed to complete the switching from the main guide to the leaky slab guide (to reach one modulation cycle, if the guide is long enough), instead the 90° rotation is required in the case of using the phase modulation (to reach the half-wave voltage). Therefore, the required voltage for this leaky modulation could be much lower.

The remaining question will be how to rotate the polarization in order to realize such an efficient intensity modulation? The answer will directly relate to the used waveguide fabrication method. It is well known that the proton exchanging (PE) will generate a significant difference for ordinary (n_o) and extraordinary (n_e) refraction indices inside the LN's index ellipsoid [8]. Normally the PE largely increases the extraordinary (n_e) index which makes the δn_e positive ($\delta n_e \sim 0.03$ to 0.15). It slightly reduces the ordinary (n_o) index which makes the δn_e slightly negative ($\delta n_e \sim -0.03$ to 0.00). Figure 5 shows a typical index variation as the wavelength of both n_o and n_e , before and after the proton exchanging [9]. Extraordinary (n_e) index corresponds to the light's polarization aligned to the LN crystal's z -axis (c-cut), and ordinary (n_o) to x -axis or y -axis (a-cut or b-cut).

Further to use a c-cut, LN SCW is an example. When the incident single-spatial-mode polarization is aligned along the crystal's z -axis, the light sees a large increase in the extraordinary (n_e) index in the main guiding layer if fabricated by the PE method. The SCW structure meets the requirement of $n_3 < n_2 < n_1$, this single-spatial-mode is optically confined and thus fully guided. If its polarization is rotated 90° and is parallel to y -axis, the light now sees an unchanged or even slightly reduced ordinary (n_o) index, when comparing to the substrate's ordinary index. In this case, this designed SCW structure no more exists and the incident light will be fully leaky to both leaky guide and substrate sides. An intensity monitoring at the main guide's output end will thus see a 0-to-100% variation. In real case, there is no need to rotate the polarization to a full 90° for

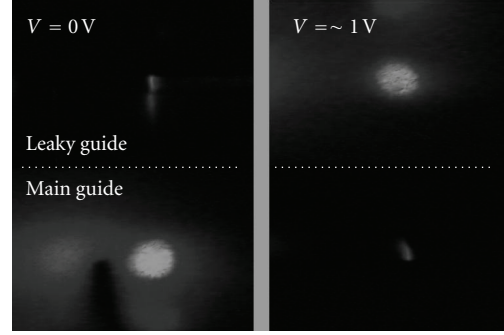


FIGURE 6: Experimental image showing intensity switching between the main and leaky waveguides by applying ~ 10 V electrical field.

reaching a full leakage. This is because that as long as it starts to leak, it will become eventually full when the electrode-applied waveguide is sufficiently long.

4. Experimental Demonstration

Fabrication of such LN SCOWs follows a procedure of a soft proton exchange (SPE) on c-cut LN crystal and then an overgrowth of thin LN film on top of the wafer, and it was introduced with details in a previous publication [10]. The final pattern formation was done by using drying etching method and standard chromium protection mask to fabricate two ridges (each $\sim 10 \mu\text{m}$ wide), which are separated by a slab with a designed width of $\sim 10 \mu\text{m}$. The waveguide was then end-polished to be $\sim 5 \text{mm}$ long. Gold electrodes were evaporated on top of the slab and the two side ridges (using the same protection mask), and the dc electrical field was applied via a pair of contacting probes.

In order to effectively rotate the polarization plane of the incident beam that was initially set parallel to the LiNbO_3 crystal's z -axis, the applied internal electric field must have an angle to the polarization plane. The electrode alignment used here (made on top of both the slab and the two ridges aside) actually uses both γ_{33} and γ_{31} EO coefficients, and is thus effective, even though it is not the optimized design.

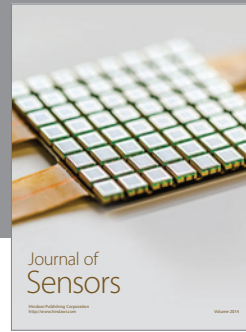
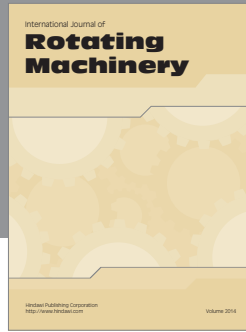
Preliminary demonstration of the switching from the main guide to the leaky guide was done by end-coupling a cw $1.55 \mu\text{m}$ Er-doped fiber laser into the main guide (vertically polarized by a polarizer), and the output was monitored by a CCD at about 1 cm away. When applying $\sim 10 \text{V}$ to the device, a clear switching was seen as shown in Figure 6. Those visible side diffractions indicate a certain level of imperfection of the fabricated waveguide, which suggests the needed effort for further improvement over both fabrication and design. The measured extinction ratio is only about 10 dB, which may be affected by those side-diffractions. We have to point out that in Figure 6 the images were taken intentionally off the best extinction status, in order to compare the two-output spots from the facet. It is also believed that the electrode voltage can be further reduced if the electrodes are made on top of the slab and inside the ditches, and by using more optimized designs and fabrications.

5. Conclusion

A new design of electro-optic intensity modulator using LN SCWs was demonstrated, in which the modulation can be realized by electrically switching the optical beam between the main waveguide and the closely attached leaky slab waveguide. Low driving voltage can be expected from using such SCW designs because of using the new leaky mechanism. The theory for simulating such LN SCWs was suggested, and the result indicates the possibility of making a large, circular, and symmetric single-spatial-mode waveguide. This allows the potential to reduce coupling losses with adjacent fiber networks. Optical modulation was experimentally demonstrated in a 5 cm long SCW waveguide fabricated using a procedure of soft proton exchange and then an overgrowth of thin LN film on top of the wafer. The used switching voltage is about 1.0 V in this preliminary design, and the result indicates the potential for further improvement.

References

- [1] A. Loayssa, D. Benito, and M. J. Garde, "Single-sideband suppressed-carrier modulation using a single-electrode electrooptic modulator," *IEEE Photonics Technology Letters*, vol. 13, no. 8, pp. 869–871, 2001.
- [2] G. H. Jin, Y. K. Zou, V. Fuflyigin, et al., "PLZT film waveguide Mach-Zehnder electrooptic modulator," *Journal of Lightwave Technology*, vol. 18, no. 6, pp. 807–812, 2000.
- [3] G. E. Betts, "LiNbO₃ external modulators and their use in high performance analog link," in *RF Photonic Technology in Optical Fiber Links*, W. S. Chang, Ed., pp. 81–129, Cambridge University Press, Cambridge, UK, 2002.
- [4] M. Sugiyama, "Hi perf LiNbO₃ modulators," in *Proceedings of the Optical Fiber Communications Conference (OFC '03)*, vol. 2, pp. 764–765, Atlanta, Ga, USA, March 2003.
- [5] J. J. Plant, P. W. Juodawlakis, R. K. Huang, J. P. Donnelly, L. J. Missaggia, and K. G. Ray, "1.5- μm InGaAsP-InP slab-coupled optical waveguide lasers," *IEEE Photonics Technology Letters*, vol. 17, no. 4, pp. 735–737, 2005.
- [6] E. A. J. Marcatili, "Slab-coupled waveguides," *Bell Labs Technical Journal*, vol. 53, no. 4, pp. 645–674, 1974.
- [7] M. R. Ramadas, E. Garmire, A. K. Ghatak, K. Thyagarajan, and M. R. Shenoy, "Analysis of absorbing and leaky planar waveguides: a novel method," *Optics Letters*, vol. 17, no. 7, pp. 376–378, 1989.
- [8] T. Tamir, *Guided-Wave Optoelectronics*, Springer, Berlin, Germany, 1990.
- [9] M. Marangoni, R. Osellame, R. Ramponi, and E. Giorgetti, "Second harmonic generation from radiation to guided modes for the characterization of reverse-proton-exchanged waveguides," *Optics Express*, vol. 12, no. 2, pp. 294–298, 2004.
- [10] Y. Lu and R. J. Knize, "Laser-assisted fabrication of new slab-coupled lithium niobate optical waveguide," *Applied Surface Science*, vol. 254, no. 4, pp. 1079–1082, 2007.



Hindawi

Submit your manuscripts at
<http://www.hindawi.com>

